Effect of particle size on the fracture toughness of epoxy resin filled with spherical silica

Yoshinobu Nakamura and Miho Yamaguchi
Central Research Laboratory, Nitto Denko Corporation, Shimohozumi, Ibaraki, Osaka, 567, Japan

and Masayoshi Okubo and Tsunetaka Matsumoto
Department of Industrial Chemistry, Faculty of Engineering, Kobe University, Nada-ku, Kobe, 657, Japan
(Received 9 January 1991; revised 25 June 1991; accepted 2 July 1991)

The effect of particle size on the fracture behaviour of cured epoxy resin filled with spherical silica particles was studied. Five kinds of spherical silica particles prepared by hydrolysis of silicon tetrachloride having different mean sizes, ranging from 6 to 42 μm, were used. The critical stress intensity factor (K_C) and the critical strain energy release rate (G_c) of the cured epoxy resins filled with the silica particles were measured. Both K_C and G_C values increased with particle size. Scanning electron microscope observation shows that the main crack propagation was hampered by large particles and a damage zone was formed at the main crack tip region in the large particle filled resin due to crack diversion and debonding of particle/matrix interfaces. The higher K_C and G_C values seem to be derived from these phenomena.

(Keywords: epoxy resin; fracture toughness; fractography)

INTRODUCTION

The drawback of epoxy resin is still its 'low toughness'. That is, cured epoxy resin is a rather brittle polymer that has poor resistance to cracking[1].

Many researchers[2–16] have improved the toughness by the addition of rigid filler particles into the epoxy matrix and have proposed some toughening mechanisms based on fracture mechanics. Most of these studies were carried out using glass beads, and a few studies used silica particles ranging from 60 to 300 μm in diameter[13]. Recently, cured epoxy resins filled with irregular shaped and spherical silica particles in the size range from submicron to about 100 μm have been used as a packaging material for integrated circuits[17,18].

In our previous articles[19–23], we have studied the effects of particle size on the fracturing, toughening[19,23], mechanical[20,22] and impact properties[19] of cured epoxy resin filled with irregular shaped silica particles in the size range from 2 to 47 μm.

In this study, the effects of particle size on the fracturing and toughening of cured epoxy resin using spherical silica particles ranging from 2 to 42 μm are investigated by the same methods employed in the previous articles[19,23].

EXPERIMENTAL

Materials

The spherical silica particles (Excelica ML-801, Tokuyama Soda Co., Ltd) were prepared as follows. Agglomerated SiO_2 was produced by hydrolysis of silicon tetrachloride through the following reaction:

$$SiCl_4 + 2H_2O \rightarrow SiO_2 + 4HCl \quad (1)$$

The agglomerated SiO_2 was then fused in a hydrogen and oxygen flame, and as a result, spherical particles were obtained. The particles were sorted into five groups in the range from 6 to 42 μm by air separation. In addition, the finest silica particles (Adoma-fine, SO-32H type, mean particle size: 2 μm, supplied by Tatsumori Ltd) prepared by fusing metallic Si powder in an oxygen flame at 4000°C (vaporize metallic conversion method) were used without sorting.

Figure 1 shows scanning electron microscope (s.e.m.) photographs of these silica particles. Their size distribution curves obtained using a laser-beam type size distribution analyser (Granulométre 715 type, Cilas Alcatel) are shown in *Figure 2*. The particle sizes at which the accumulated distribution values reached 50% were defined as the mean particle size and are shown near the corresponding curves in *Figure 2*.

The epoxy resin used was bisphenol A type epoxy resin (Epikote 828, Shell Chemical Co., equivalent weight per epoxy group: 190 ± 5, average molecular weight: 380). Hexahydrophthalic anhydride and tri-n-butylamine were used as hardener and accelerator for curing the epoxy resin, respectively.

Sample preparation

Table 1 shows the formulations of the epoxy resin filled with silica particles. Silica particles were dispersed in the

0032-3861/92/163415-12

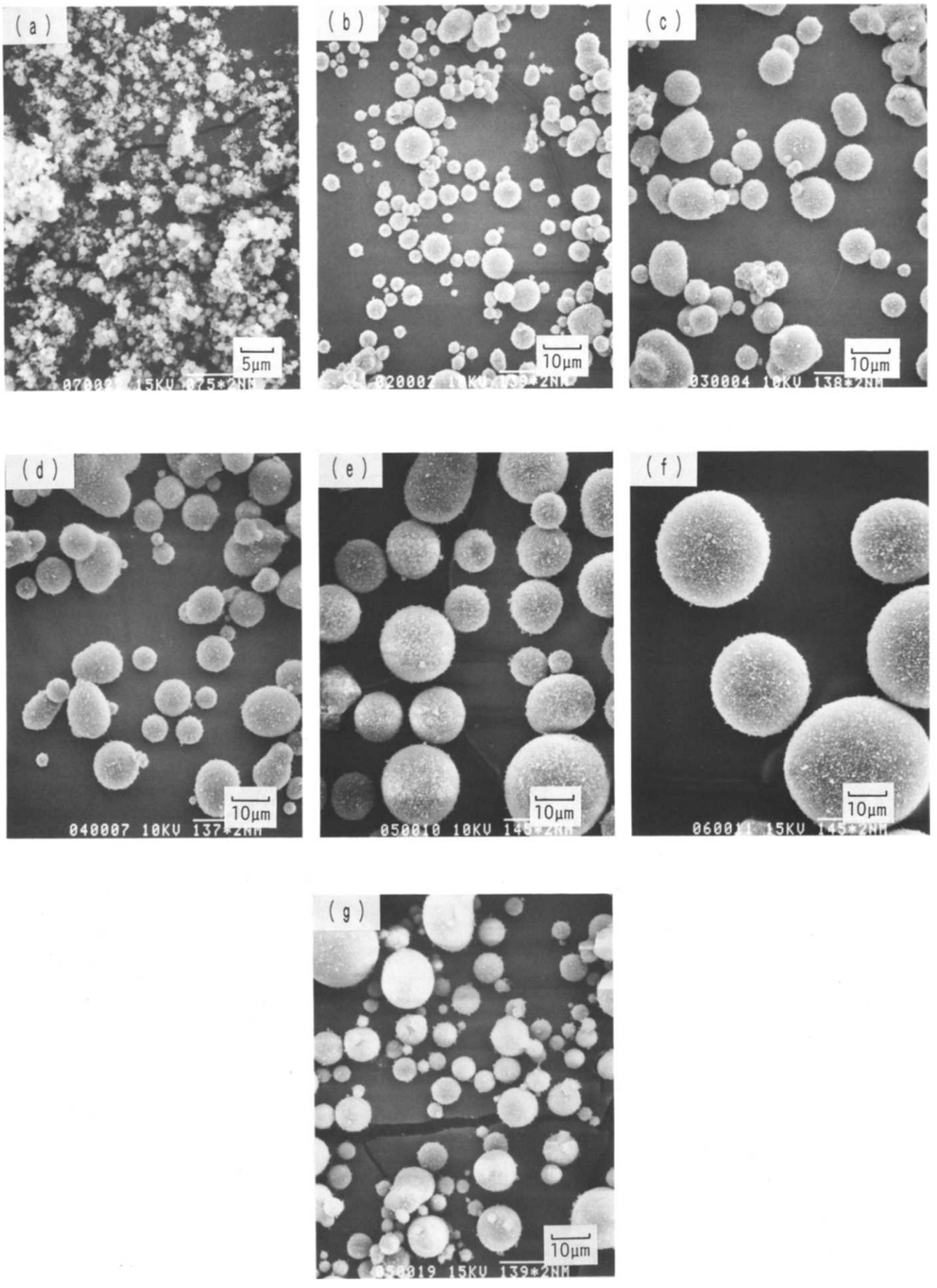

Figure 1 S.e.m. photographs of unsorted (a, g) and sorted (b–f) spherical silica particles having different mean particle sizes. Mean particle size: (a) 2 μm; (b) 6 μm; (c) 13 μm; (d) 17 μm; (e) 24 μm; (f) 42 μm; (g) 25 μm

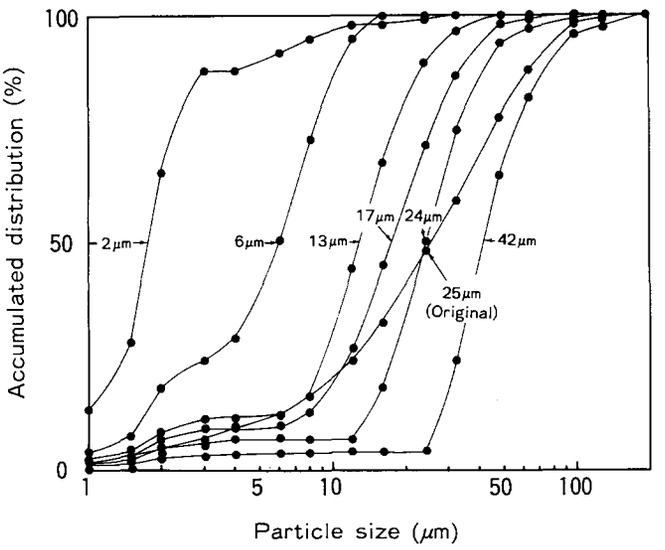

Figure 2 Accumulated particle size distribution curves for unsorted and sorted spherical silica particles. The numbers written near corresponding curves show their mean particle size

Table 1 Formulations of epoxy resin filled with silica particles[a]

	Unfilled	Filled with particles	
Particle content (wt%)	0	55	64
Epoxy resin[b]	60.06	27.03	21.62
Hardener[c]	39.64	17.83	14.27
Accelerator[d]	0.30	0.14	0.11
Silica particles[e]	–	55.00	64.00

[a]Unit: wt%
[b]Bisphenol A type epoxy resin (Epikote 828)
[c]Hexahydrophthalic anhydride
[d]Tri-n-butylamine
[e]Irregular shaped silica particles

mixture of epoxy resin and hardener by stirring at room temperature for 1 h, under vacuum degassing. The accelerator was added to the mixture under stirring for 10 min. The final mixture was cured in a mould (4 × 10 mm, height: 100 mm, 4 × 50 mm, height: 140 mm, and 10 × 10 mm, height: 140 mm) at 120°C for 2 h, followed by 140°C for 21 h.

Fracture studies

The critical stress intensity factor (fracture toughness, K_C) and critical strain energy release rate (fracture energy, G_C) at static speed were measured by both a single edge notched beam loaded in three-point bending (SENB) test[19,26] and a double torsion (DT) test[9–11,19,28]. Those values at impact speed (K_{CI} and G_{CI}, where I in the subscripts means impact) were also measured by the impact fracture toughness test[23,31,33–36].

SENB test. The shape and dimension of the SENB test specimen employed in this study are shown in *Figure 3*. An acute incision was introduced at the base of the slot of the test specimen maintained at 110°C using a fresh razor blade (Microtome knives, T-40 type, Nippon Microtome Laboratory Co., Ltd). It was observed using an optical microscope after the fracture test that a short starter crack had formed ahead of the acute incision[19].

The load–time curve was measured with a displacement rate of 10 mm min^{-1} at room temperature.

K_C was calculated from

$$K_C = \frac{3P_C S}{2BW^2}\sqrt{a}\,f(x) \qquad (2)$$

where P_C is the load at fracture, a is the crack length, W is the specimen width, B is the specimen thickness, S is the support span and $f(x)$ is a geometric factor given by

$$f(x) = 1.93 - 3.07x + 14.53x^2 - 25.11x^3 + 25.80x^4 \qquad (3)$$

where $x = a/W$. The above procedures and the measurement of G_C are explained in detail in a previous article[19], and were according to ASTM[26,27] and others[28,29].

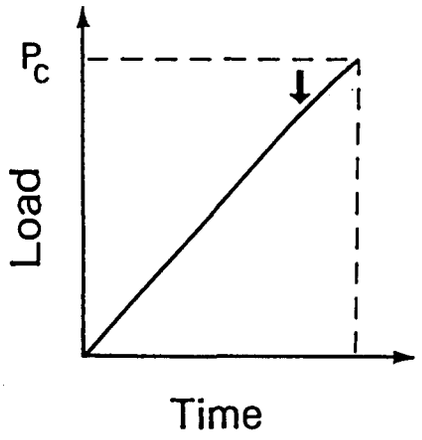

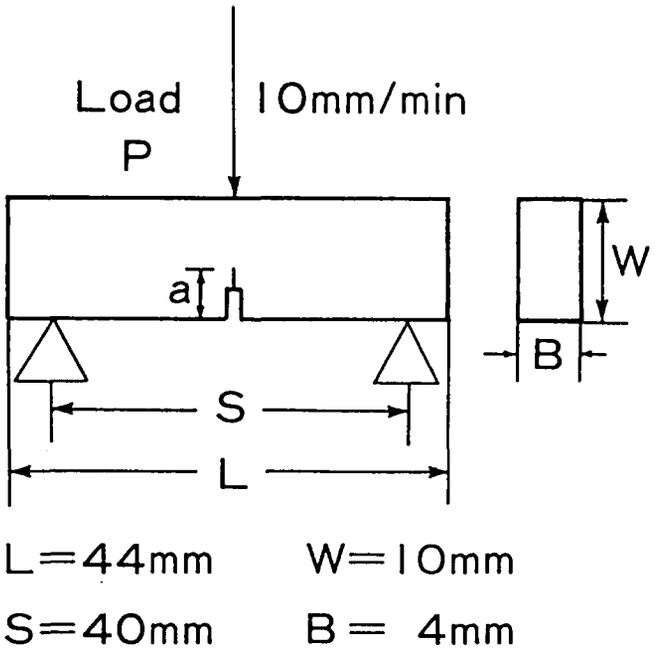

Figure 3 Shape and dimension of SENB (single edge notched beam loaded in three-point bending) fracture toughness test specimen and its typical load–time curve. The arrow in the load–time curve indicates the inflection point from elastic deformation

DT test. The shape and dimensions of the DT test specimen employed in this study and the test procedures were described in detail in the previous article[19]. The sizes were 4 × 50 × 100 mm. The specimen had a notch and a V-shaped groove which was machined along the notch. The depth of the groove was 0.5 mm. An acute incision was introduced at the base of the slot using the same method as for the SENB test explained above. P_C was measured at the displacement rate of 0.5 mm min^{-1}.

K_C was calculated from:

$$K_C = P_C W_m \left\{ \frac{3}{W d^3 d_n (1-\nu) \xi} \right\}^{1/2} \quad (4)$$

$$\xi = 1 - 5d/4W \quad (5)$$

where P_C is the load for the propagating crack, W_m is the moment arm, W is the specimen width, d is the specimen thickness, d_n is the specimen thickness at the bottom of the groove and ν is Poisson's ratio (= 0.33).

G_C was calculated from:

$$G_C = \frac{K_C^2}{E}(1-\nu^2) \quad (6)$$

where E is the Young's modulus measured by flexural testing. The results for mechanical properties containing these E values will be explained in detail in a following article[24].

Impact fracture toughness test. The procedures of the impact fracture toughness test were described in detail in the previous article[23]. The sizes of the specimens were 10 × 10 × 90 mm, with a slot of various lengths (1–2.5 mm). An acute incision was introduced at the base of the slot using the same method as for the SENB test explained above. The total crack length, a, was measured by an optical microscope after the test. The support span was 60 mm. The impact fracture toughness test was carried out using the instrumented Charpy type impact tester[21,23,32–36] (CAI-AC5-CZ(A) type, Japan Sensor Corp., Capacity: 14.7 J) described in detail in previous articles[21,23]. This tester can record a load–displacement curve of impact fracture. The hammer speed at strike was 1.10 m s^{-1}. The impact fracture load (P_{CI}) and the impact absorbed energy (U) were measured from the load–displacement curve as explained in detail in previous articles[21,23].

K_{CI} was calculated from equations (2) and (3) using P_{CI}. G_{CI} was measured by the method employed by Plati and Williams[34] and Ting and Cottington[33]. The linear relation between G_{CI} and U is shown as follows:

$$U = G_{CI} B W \phi \quad (7)$$

where B and W are specimen thickness and width, respectively, and ϕ is a dimensionless factor given by

$$\phi = \frac{C}{\mathrm{d}C/\mathrm{d}(a/W)} \quad (8)$$

where C is compliance.

Fractography and observation of the crack tip region

Figure 4 shows schematic views of the original SENB specimen (a), and of those observed by s.e.m. (b, c). The squares show the areas observed. The starter crack tip region of the surface of the fractured SENB specimen was observed as shown in *Figure 4b*. The vertical view for the starter crack tip region of the SENB specimen before testing was observed as shown in *Figure 4c*. In this case, the specimen was cut in half vertically and the exposed surface was polished by the method explained in a previous article[19].

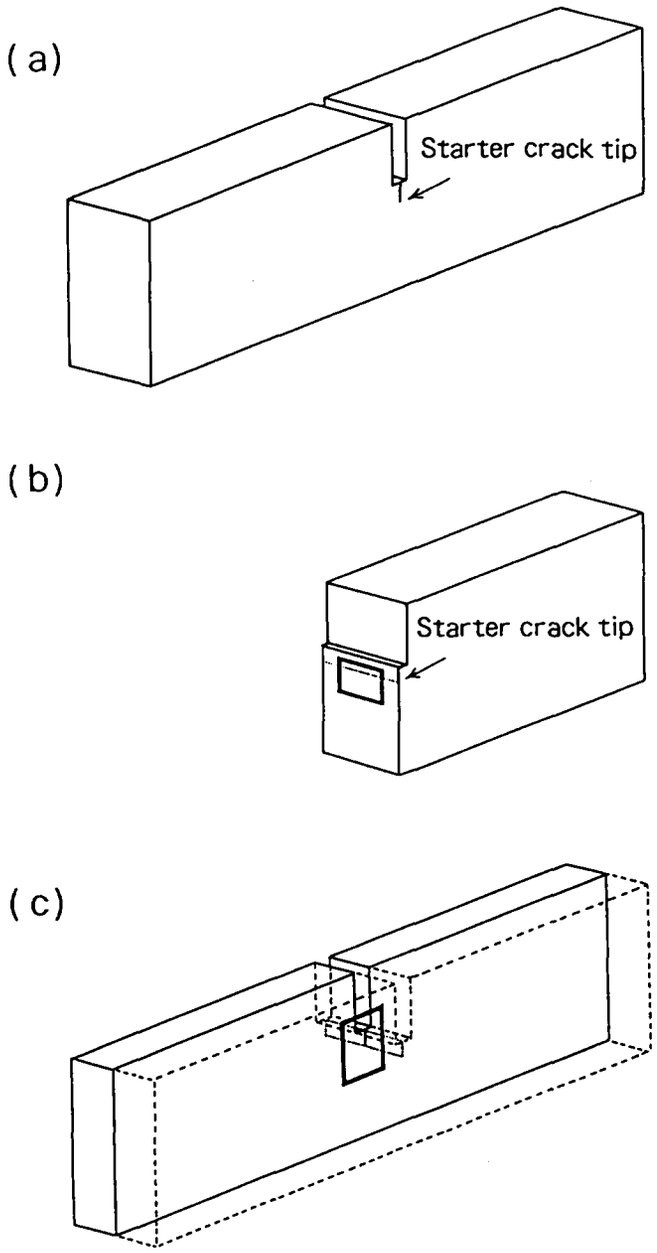

Figure 4 Observed parts for SENB specimens of before and after test: (a) SENB specimen; (b) fractured specimen after test; (c) vertically cut specimen before test. The parts enclosed by squares show the parts observed by s.e.m.

RESULTS AND DISCUSSION

Figure 5 shows s.e.m. photographs of the polished surfaces of cured epoxy resins filled with unsorted original (a, g) and sorted (b–f) spherical silica particles at particle contents of 55 wt% (a) and 64 wt% (b–g). These indicate that the particles were well dispersed in the cured epoxy matrix. In the larger particle filled resins (e, f), the particle content between the upper part and the bottom part of the specimen in the mould was

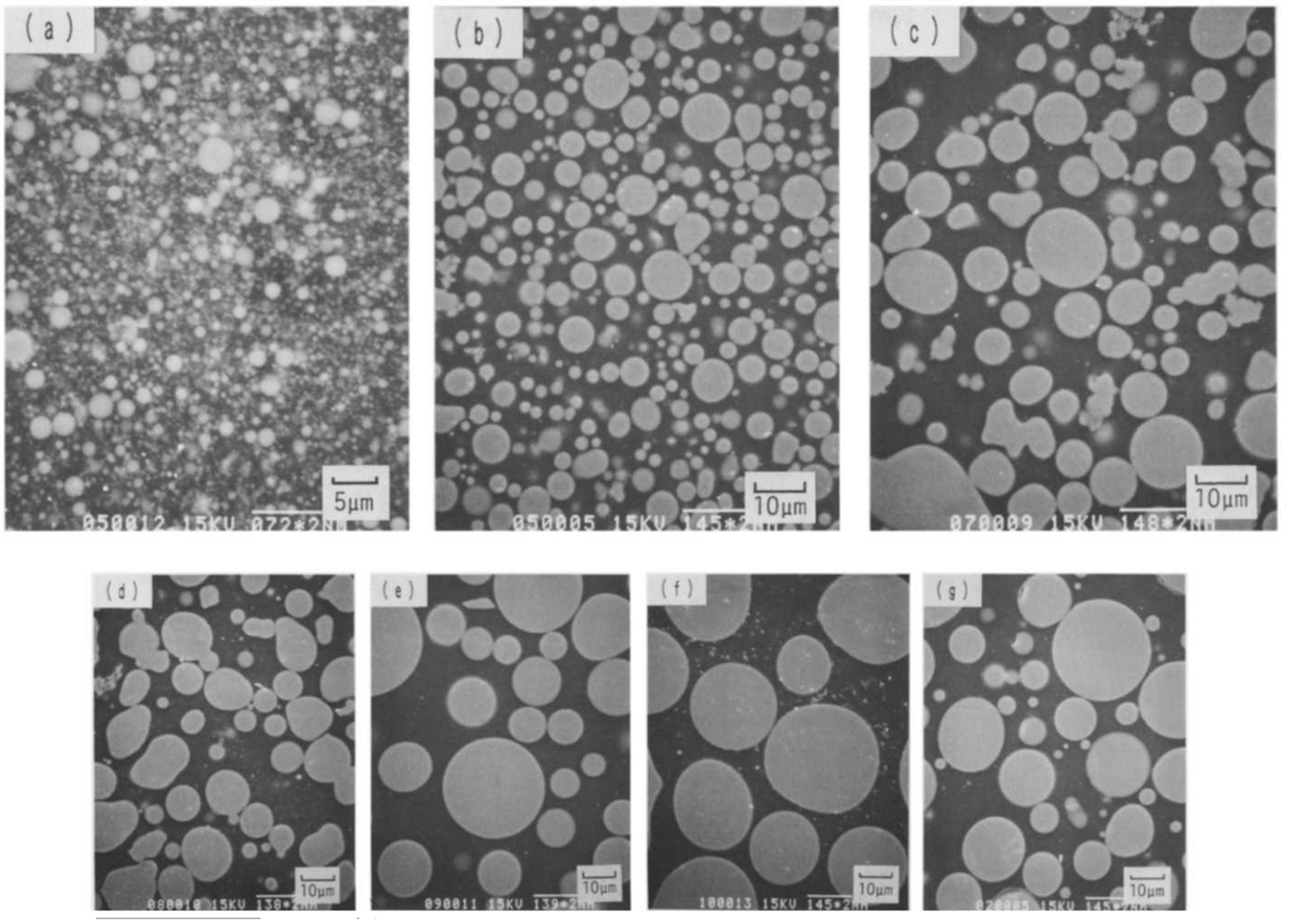

Figure 5 S.e.m. photographs of the polished surfaces of curved epoxy resins filled with unsorted (a, g) and sorted (b–f) spherical silica particles for particle contents of 55 wt% (a) and 64 wt% (b–g). Mean particle size of filled silica: (a) 2 μm; (b) 6 μm; (c) 13 μm; (d) 17 μm; (e) 24 μm; (f) 42 μm; (g) 25 μm

different, because of sedimentation of the particles during curing. However, since particle contents of the fractured parts of all specimens obtained from the measurement of specific gravity were almost equal to the particle contents in the corresponding specimens, the influence of sedimentation is neglected in the following discussion.

Figures 6 and *7* show the effects of particle size on K_C and G_C values measured by the SENB test of the cured epoxy resin filled with these particles, respectively. K_C and G_C values increased with increasing particle size.

Figures 8 and *9* show the K_C and G_C values measured by the DT test, respectively. With increasing particle size, K_C and G_C values increase as well as those measured by the SENB test shown in *Figures 6* and *7*.

Figures 10 and *11* show the K_{CI} and G_{CI} values measured by the impact test, respectively. K_{CI} and G_{CI} values also increased with increasing particle size.

The results obtained from *Figures 6–11* indicate that the addition of larger spherical silica particles increased the toughness of the cured epoxy resin, at the same

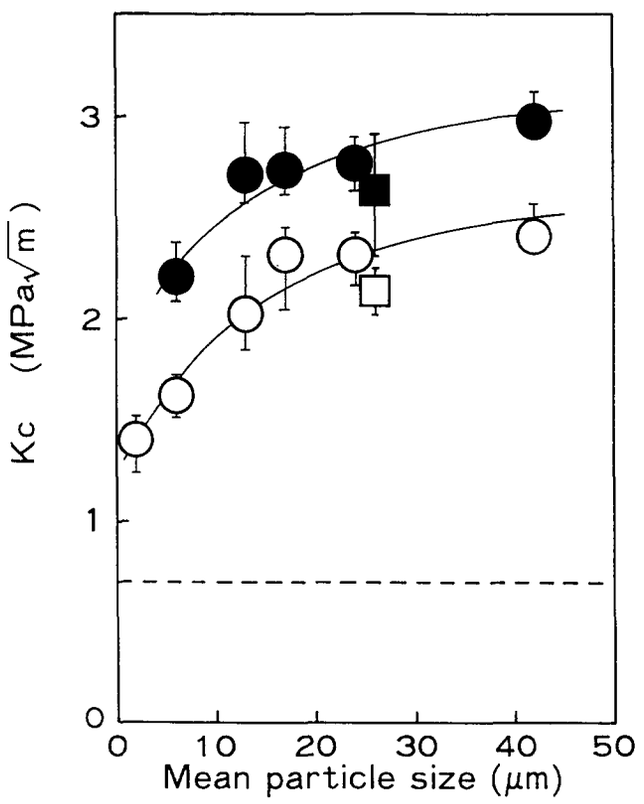

Figure 6 Effect of particle size on critical stress intensity factor (K_C) measured by SENB test of cured epoxy resins filled with unsorted (□, ■) and sorted (○, ●) spherical silica particles with particle contents of 55 wt% (□, ○) and 64 wt% (■, ●). Broken line indicates the K_C value of unfilled cured epoxy resin

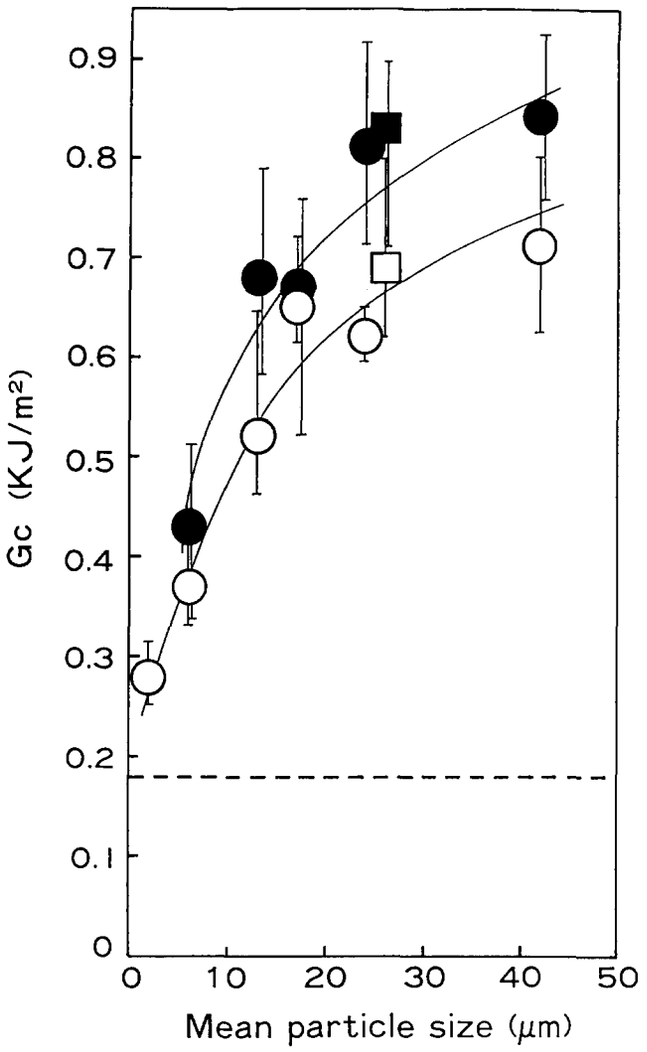

Figure 7 Effect of particle size on critical strain energy release rate (G_C) measured by SENB test of cured epoxy resins filled with unsorted (□, ■) and sorted (○, ●) spherical silica particles with particle contents of 55 wt% (□, ○) and 64 wt% (■, ●). Broken line indicates the G_C value for unfilled cured epoxy resin

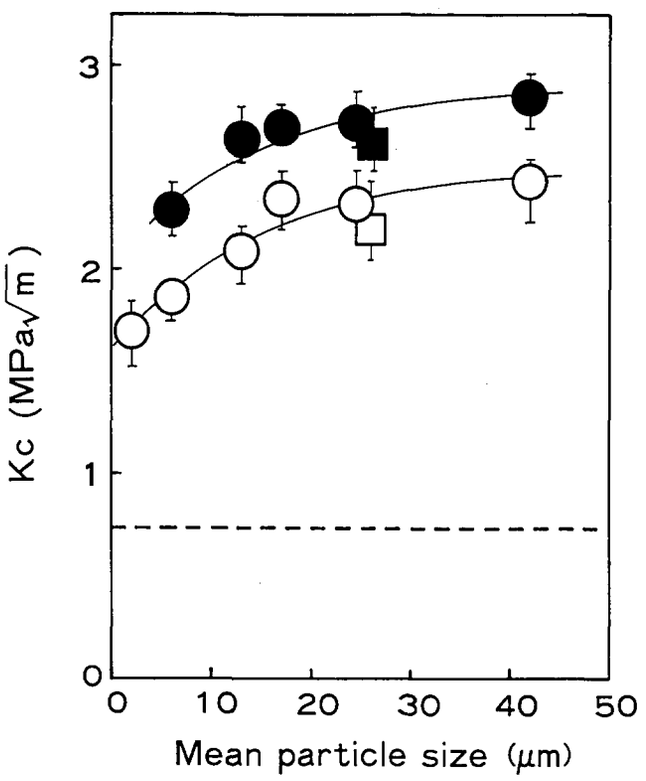

Figure 8 Effect of particle size on critical stress intensity factor (K_C) measured by DT test of cured epoxy resins filled with unsorted (□, ■) and sorted (○, ●) spherical silica particles with particle contents of 55 wt% (□, ○) and 64 wt% (■, ●). Broken line indicates the K_C value for unfilled cured epoxy resin

particle content, although the extent of the increases of both K_C and G_C measured by the DT test and K_{CI} and G_{CI} measured by the impact test with increasing particle size (*Figures 8–11*) was smaller than those measured by the SENB test (*Figures 6* and *7*). These phenomena were in accordance with the results obtained in the cured epoxy resin filled with irregular shaped silica particles having similar sizes reported in previous articles[19,23].

The fractured surfaces were then observed. It has already been reported that a slow propagated crack was observed ahead of the starter crack tip in the fractured SENB specimen[28,29], as schematically shown in *Figure 12*.

Figure 13 shows the slow (a, b) and fast (c, d) propagated crack in fractured SENB specimens observed by s.e.m. as shown in *Figure 4b*. The arrows in *Figures 13a* and *b* indicate the starter crack tip. In the small particle filled resin (mean size: 6 μm, *Figures 13a* and *c*), the surfaces were relatively smooth and there was no difference between the slow (*Figure 13a*) and the fast propagated crack (*Figure 13c*). However, in the largest particle filled resin (mean size: 42 μm, *Figures 13b* and *d*), the surfaces were rough and there was a significant

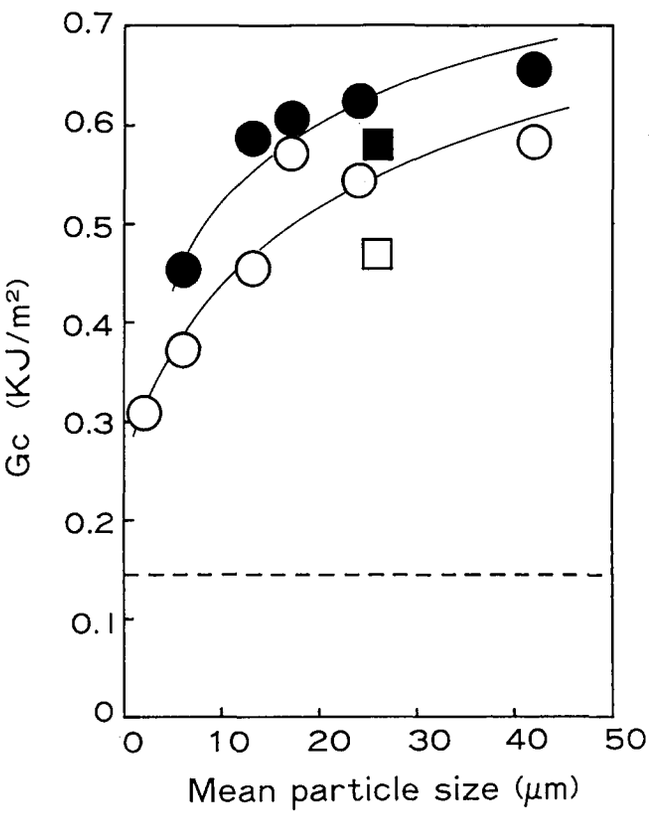

Figure 9 Effect of particle size on critical strain energy release rate (G_C) measured by DT test of cured epoxy resins filled with unsorted (□, ■) and sorted (○, ●) spherical silica particles with particle contents of 55 wt% (□, ○) and 64 wt% (■, ●). Broken line indicates the G_C value for unfilled cured epoxy resin

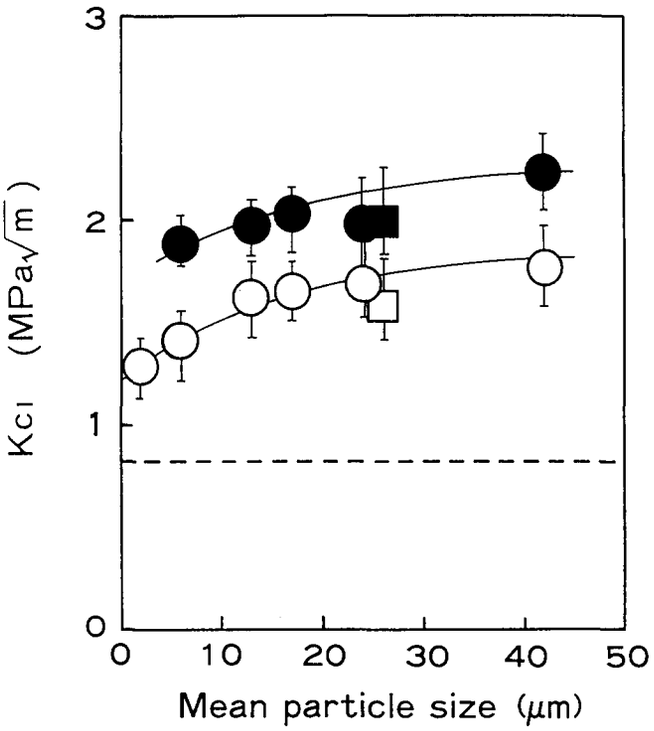

Figure 10 Effect of particle size on impact critical stress intensity factor (K_{CI}) measured by impact fracture toughness test of cured epoxy resins filled with unsorted (□, ■) and sorted (○, ●) spherical silica particles with particle contents of 55 wt% (□, ○) and 64 wt% (■, ●). Broken line indicates the K_{CI} value for unfilled cured epoxy resin

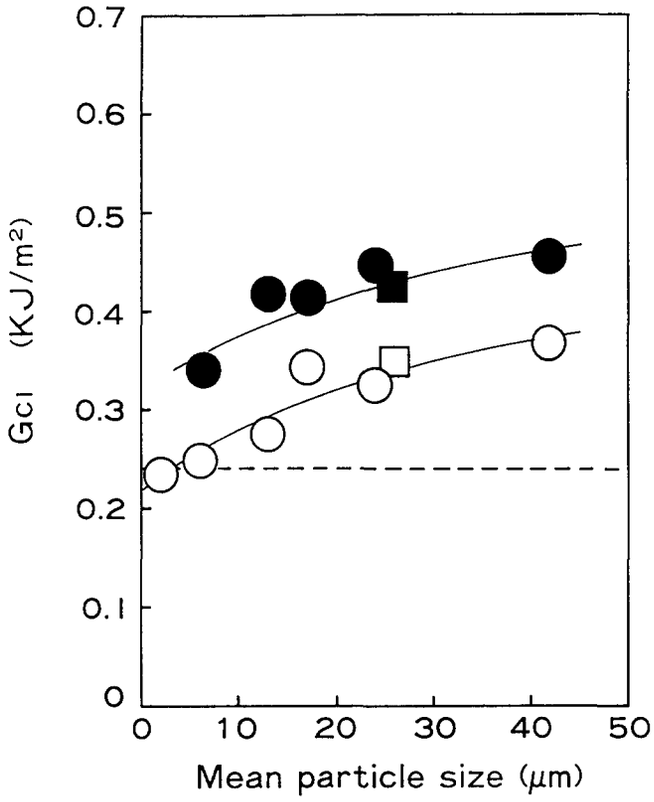

Figure 11 Effect of particle size on impact critical strain energy release rate (G_{CI}) measured by impact fracture toughness test of cured epoxy resins filled with unsorted (□, ■) and sorted (○, ●) spherical silica particles with particle contents of 55 wt% (□, ○) and 64 wt% (■, ●). Broken line indicates the G_{CI} value for unfilled cured epoxy resin

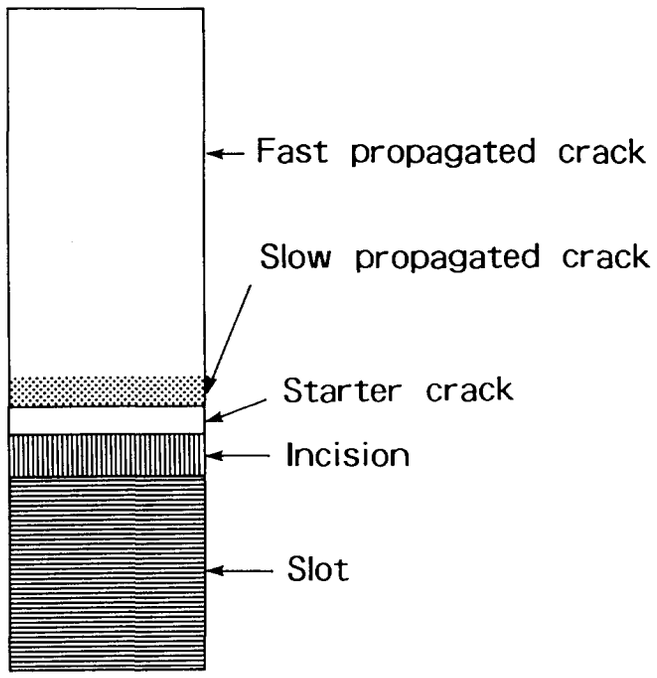

Figure 12 Schematic view of SENB specimen's fractured surface

difference between the slow (*Figure 13b*) and the fast propagated crack (*Figure 13d*). The slow propagated crack propagated around the particle/matrix interface, while the fast propagated crack propagated through the matrix. The same observation was carried out for impact test specimens after testing. However, the typical slow propagation region mentioned above was not observed.

Figure 14 shows s.e.m. photographs of polished exposed surfaces for the starter crack tip region of vertically cut SENB specimens observed before the test as shown in *Figure 4c*. Magnified sections of *Figures 14a* and *c* are shown in *Figures 14b* and *d*, respectively. In the small particle filled resin (*Figures 14a* and *c*), the starter crack tip was acute and single. In the largest particle filled resin (*Figures 14b* and *d*), however, it was not so acute and some diverging cracks were observed along the particle/matrix interface and in the cured epoxy matrix. These indicate that the condition of the starter crack was affected by the particle size. That is, the formation of an acute starter crack was hampered by the large particles. Since the diverging of the starter crack disperses the stress concentrated at the crack tip, it requires more energy for initiating a crack than the acute single crack. The same observation was obtained in the impact test specimens before test.

In the SENB test, an inflection point from elastic deformation (arrow in the upper part of *Figure 3*) was observed. Above this point, any energy absorption due to slow crack propagation or non-elastic deformation seems to be caused at the starter crack tip. In order to clarify this, polished exposed surfaces for the crack tip region of vertically cut SENB specimens which were loaded at 80% of P_C were observed by s.e.m., as shown in *Figure 4c*.

Figure 15 shows the micrographs. Magnified sections of *Figures 15a* and *c* are shown in *Figures 15b* and *d*, respectively. In the small particle filled resin (*Figures 15a* and *b*), the observed crack tip was similar to its starter crack shown in *Figures 14a* and *b*. In the largest particle

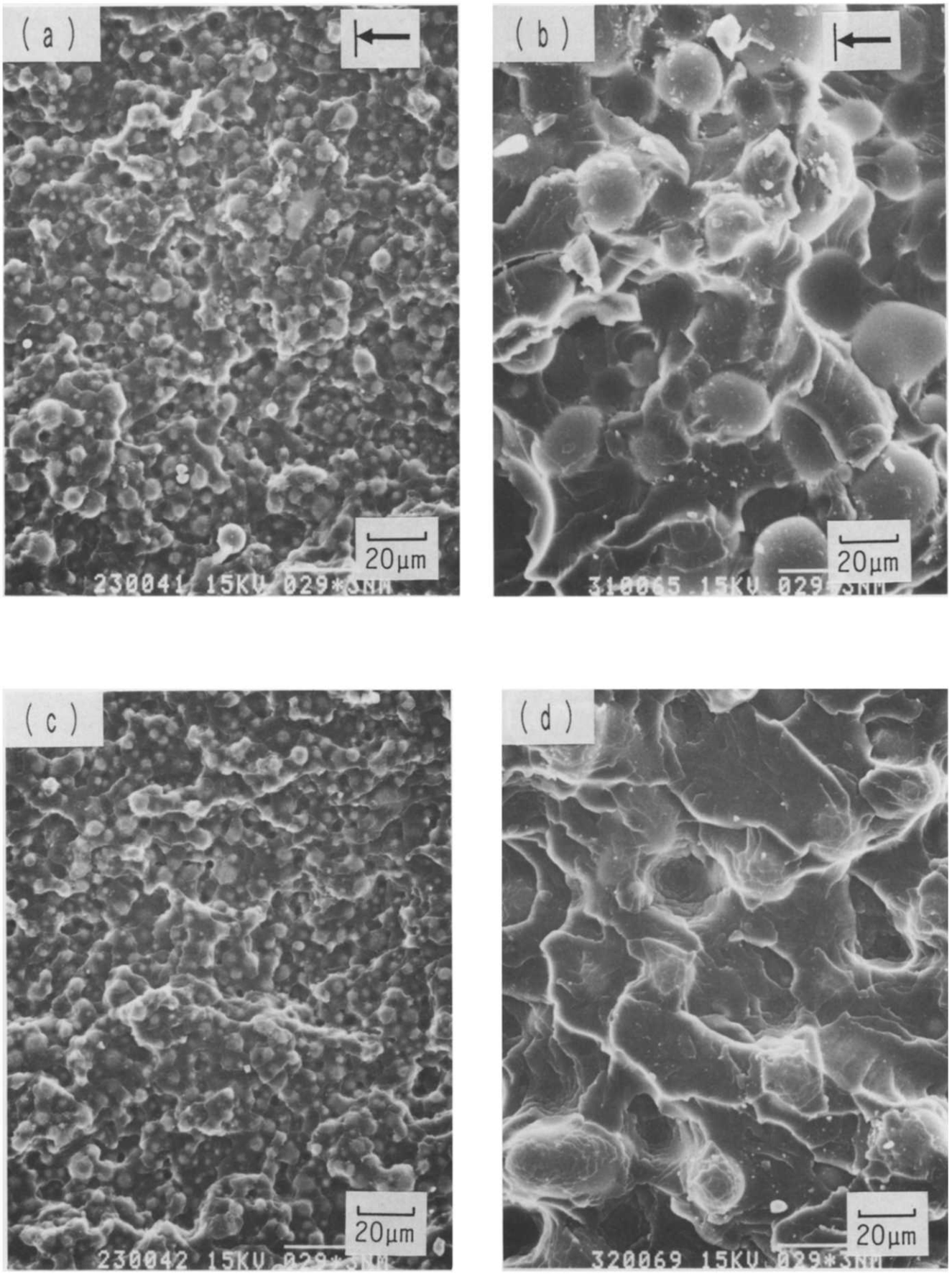

Figure 13 Slow propagated crack (a, b) and fast propagated crack (c, d) regions for surfaces of fractured SENB specimens observed by s.e.m. of cured epoxy resins filled with spherical silica particles with a particle content of 64 wt%. Mean particle size of filled silica: (a, c) 6 μm; (b, d) 42 μm. Arrow indicates the starter crack tip. The observed area is shown in *Figure 4b*

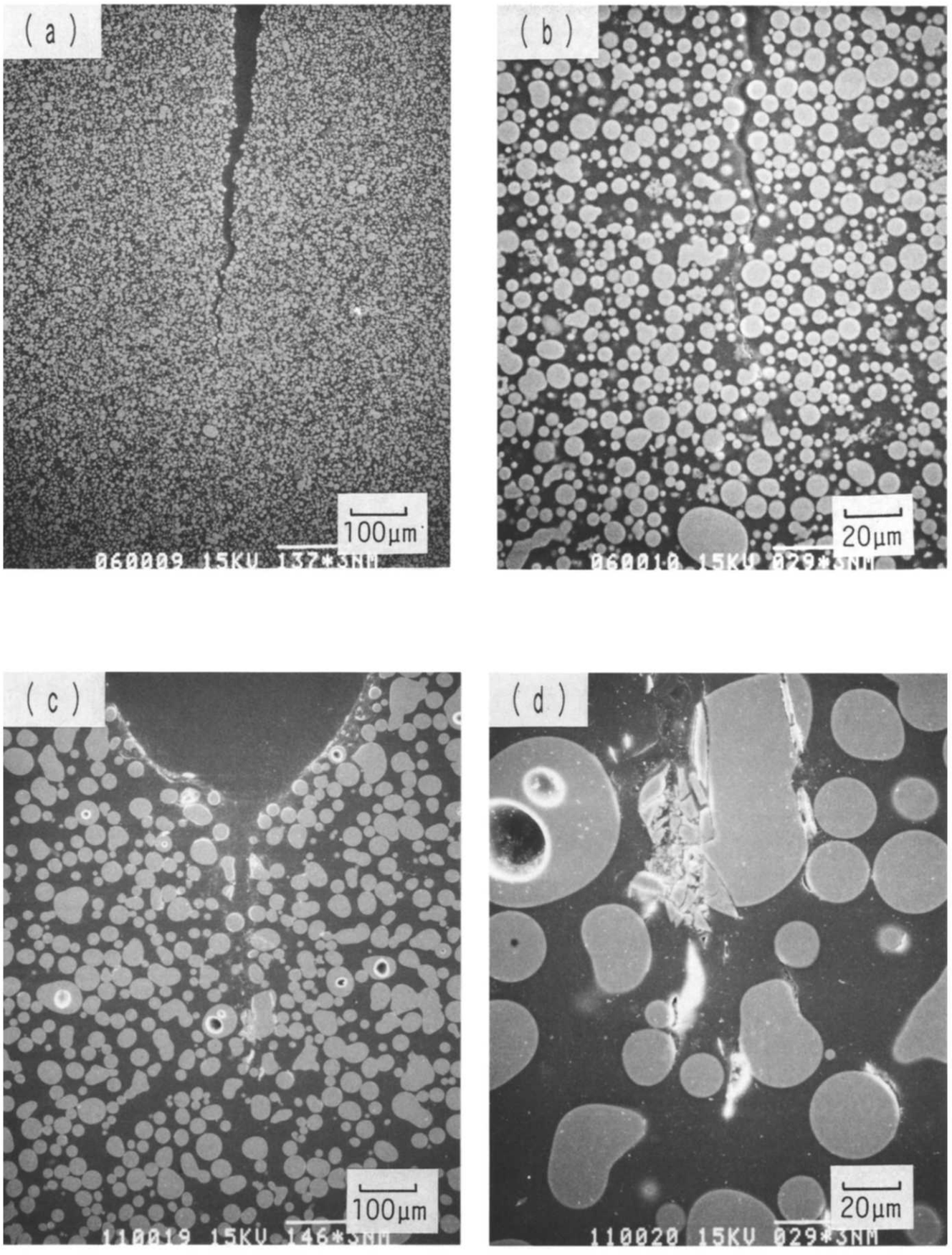

Figure 14 Polished cut-away surfaces showing starter crack tip region of vertically cut SENB specimens observed by s.e.m. of cured epoxy resins filled with spherical silica particles with a particle content of 64 wt%. Mean particle size of filled silica: (a, b) 6 μm, (c, d) 42 μm. The observed area is shown in *Figure 4c*

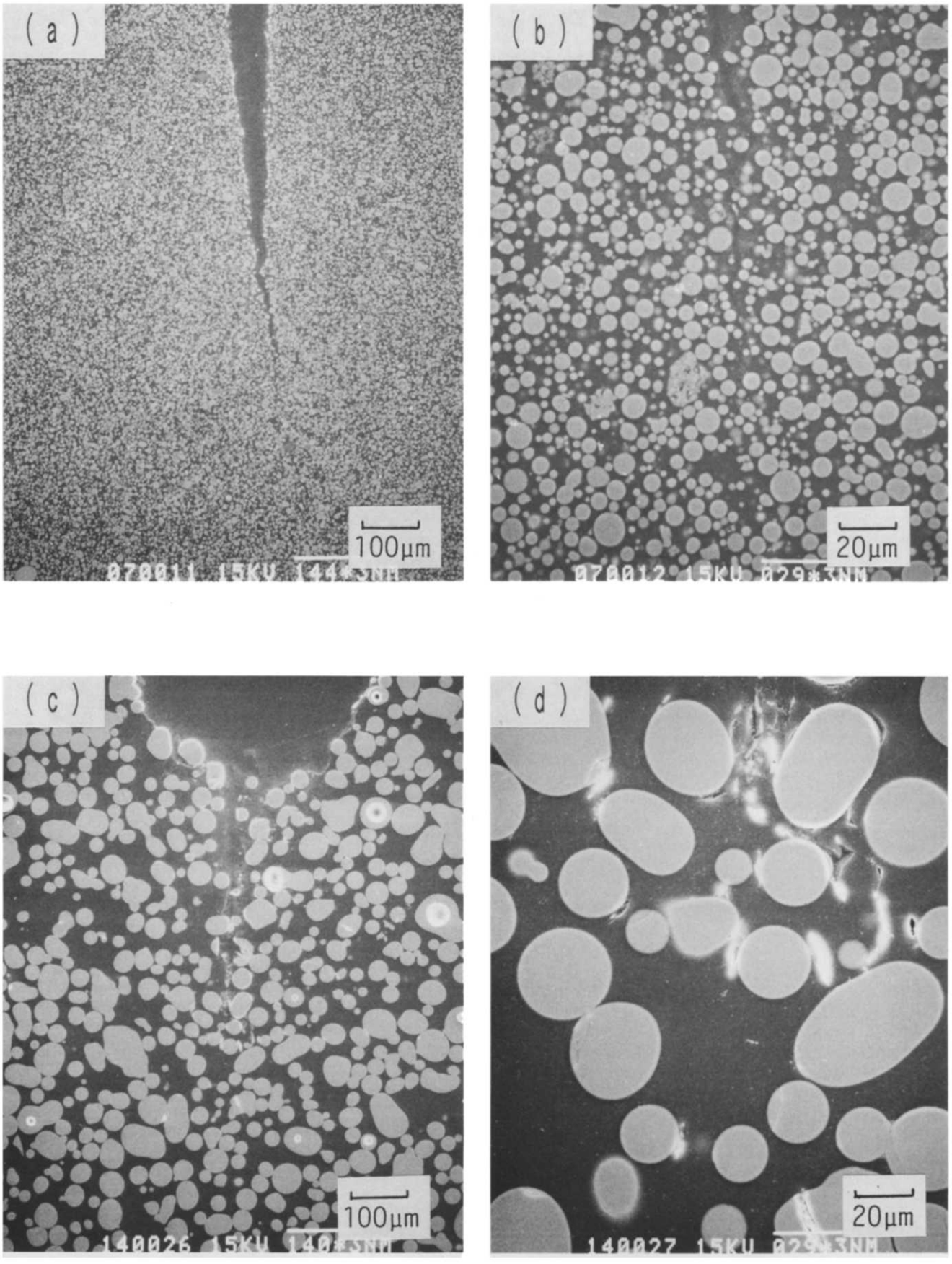

Figure 15 Polished cut-away surface showing crack tip region of vertically cut SENB specimens which were loaded and stopped at 80% of the fracture load observed by s.e.m. of cured epoxy resins filled with spherical silica particles with a particle content of 64 wt%. Mean particle size of filled silica: (a, b) 6 μm, (c, d) 42 μm. The observed area is shown in *Figure 4c*

filled resin (*Figures 15c* and *d*), however, many diverging cracks in the cured epoxy matrix and in the debonded particle/matrix interfaces were observed ahead of the starter crack tip region in a wider area. This area is called the 'damage zone[16,37]' or 'process zone[15,16]'. In the largest particle (mean size: 42 μm) filled resin, it is clear that the damage zone was larger in the loaded specimen (*Figures 15c* and *d*) than in the unloaded specimen (the starter crack tip, *Figures 14c* and *d*). However, in the small particle (mean size: 6 μm) filled resin, a damage zone was not observed in either the unloaded (starter crack tip, *Figures 14a* and *b*) or the loaded (*Figures 15a* and *b*) specimens. The formation of a damage zone due to crack diversion and debonding of the particle/matrix interface should partially absorb the stored strain energy at the crack tip and hamper crack propagation.

On the basis of the above results, the effect of the size of filled spherical silica particles on toughness is schematically shown in *Figure 16*. *Figures 16a* and *b* show the starter crack and *Figures 16a'* and *b'* show the slow propagating crack.

As described above, the increases of both K_C and G_C values measured by the DT test (*Figures 8* and *9*) with increasing particle size were smaller than those measured by the SENB test (*Figures 6* and *7*). This suggests that the effect of the diversion of the starter crack in the large particle filled resin (as shown in *Figure 16b*) on both K_C and G_C values is stronger in the SENB test than in the DT test. Furthermore, the increases of both K_{CI} and G_{CI} values measured by the impact fracture toughness test (*Figures 10* and *11*) with increasing particle size were also smaller than the K_C and G_C values measured by the SENB test. This suggests that the energy absorption by the formation of a damage zone in the large particle filled resin (as shown in *Figures 16b'*) is larger in the SENB test than in the impact fracture toughness test.

As mentioned above, the energy absorption due to the debonding of the particle/matrix interface in the slow propagated crack region in the large particle filled resin affected toughness. Therefore, the adhesion of that interface must be important in improving toughness. In a subsequent article, this point will be discussed using surface treatment by a silane coupling agent for the same silica particles.

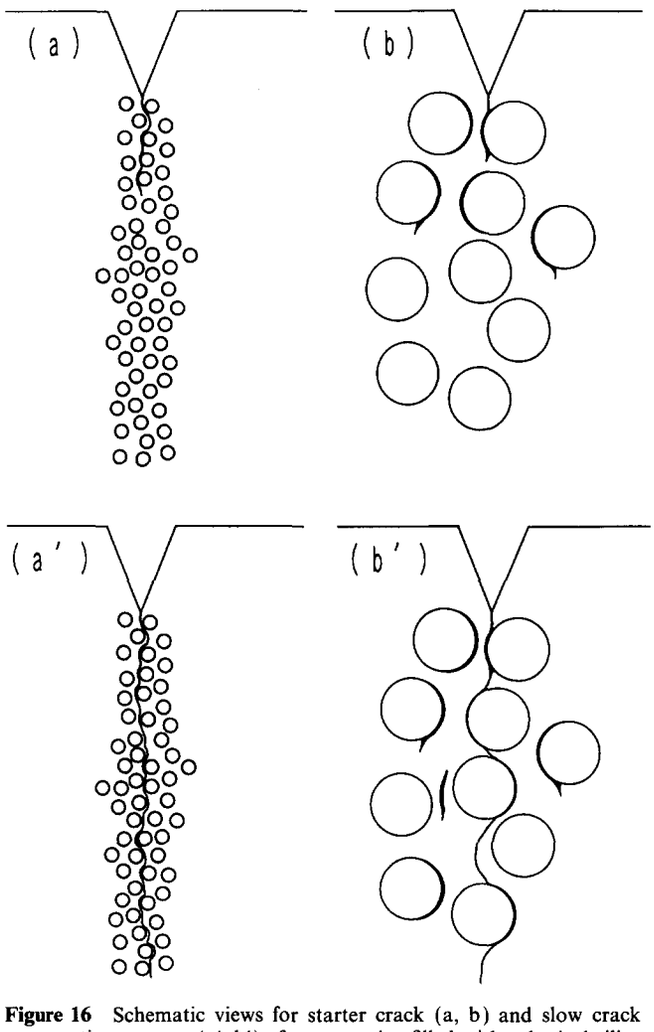

Figure 16 Schematic views for starter crack (a, b) and slow crack propagation process (a', b') of epoxy resins filled with spherical silica particles. Particle size: (a, a') small, (b, b') large

ACKNOWLEDGEMENT

The authors are grateful to Tokuyama Soda Co. Ltd and Tatsumori Ltd for the preparation of the sample silica particles.

REFERENCES

1 Moloney, A. C., Kausch, H. H., Kaiser, T. and Beer, H. R. *J. Mater. Sci.* 1987, **22**, 381
2 Faber, K. T. and Evans, A. G. *Acta Metall.* 1983, **31**, 565
3 Lange, F. F. *Phil. Mag.* 1970, **22**, 983
4 Evans, A. G. *Phil. Mag.* 1972, **26**, 1327
5 Green, D. J., Nicholson, P. S. and Embery, J. D. *J. Mater. Sci.* 1979, **14**, 1657
6 Broutsman, L. J. and Sahu, S. *Mater. Sci. Eng.* 1971, **8**, 98
7 Sahu, S. and Broutsman, L. J. *Polym. Eng. Sci.* 1972, **12**, 97
8 Owen, A. B. *J. Mater. Sci.* 1979, **14**, 2523
9 Beaumont, P. W. R. and Young, R. J. *J. Mater. Sci.* 1975, **10**, 1334
10 Young, R. J. and Beaumont, P. W. R. *J. Mater. Sci.* 1975, **10**, 1343; 1977, **12**, 684
11 Spanoudakis, J. and Young, R. J. *J. Mater. Sci.* 1984, **19**, 473, 487
12 Su, K. B. and Suh, N. P. *Soc. Plastics Eng.* 1981, **27**, 46
13 Moloney, A. C., Kausch, H. H. and Stieger, H. R. *J. Mater. Sci.* 1983, **18**, 208
14 Moloney, A. C., Kausch, H. H. and Stieger, H. R. *J. Mater. Sci.* 1984, **19**, 1125
15 Cantwell, W. J., Smith, J. W., Kausch, H. H. and Kaiser, T. *J. Mater. Sci.* 1990, **25**, 633
16 Narisawa, I. *Kobunshi Ronbunsyu* 1988, **45**, 683
17 Nishimura, A., Tatemichi, A., Miura, H. and Sakamoto, T. *IEEE Trans. Components, Hybrids, Manuf. Technol.* 1987, **CHMT-12**, 637
18 Kinjo, N., Ogata, M., Nishi, K. and Kaneda, A. *Adv. Polym. Sci.* 1989, **88**, 1
19 Nakamura, Y., Yamaguchi, M., Kitayama, A., Okubo, M. and Matsumoto, T. *Polymer* 1991, **32**, 2221
20 Nakamura, Y., Yamaguchi, M., Okubo, M. and Matsumoto, T. *J. Appl. Polym. Sci.* 1992, **44**, 151
21 Nakamura, Y., Yamaguchi, M., Okubo, M. and Matsumoto, T. *Polymer* 1991, **32**, 2979
22 Nakamura, Y., Yamaguchi, M., Okubo, M. and Matsumoto, T. *J. Thermosetting Plastics, Japan* 1991, **12**, 1
23 Nakamura, Y., Yamaguchi, M. and Okubo, M. *Polym. Eng. Sci.* in press
24 Nakamura, Y., Yamaguchi, M., Okubo, M. and Matsumoto, T. *J. Appl. Polym. Sci.* in press
25 Kinloch, A. J. and Young, R. J. 'Fracture Behaviour of Polymers', Elsevier Applied Science, London and New York, 1983, p. 74
26 ASTM Committee D-20 on Mechanical Testing, Project No. X-10-128
27 ASTM E399-81

28 Yee, A. F. and Pearson, R. A. *J. Mater. Sci.* 1986, **21**, 2462
29 Pearson, R. A. and Yee, A. F. *J. Mater. Sci.* 1986, **21**, 2475
30 Tait, R. B., Fry, P. R. and Garrett, G. G. *Exp. Mech.* 1987, **27**, 14
31 Kinloch, A. J. and Young, R. J. 'Fracture Behaviour of Polymers', Elsevier Applied Science, London and New York, 1983, p. 183
32 Kobayashi, T., Koide, Y., Daicho, Y. and Ikeda, R. *Eng. Fract. Mech.* 1987, **28**, 21
33 Ting, R. Y. and Cottington, R. L. *J. Appl. Polym. Sci.* 1980, **25**, 1815
34 Plati, E. and Williams, J. G. *Polym. Eng. Sci.* 1975, **15**, 470
35 Kinloch, A. J., Kodokian, G. A. and Jamarani, M. B. *J. Mater. Sci.* 1987, **22**, 4111
36 Narisawa, I., Ishikawa, M., Sato, K. and Saikawa, T. *Kobunshi Ronbunsyu* 1988, **45**, 139
37 Pearson, R. A. and Yee, A. F. *J. Mater. Sci.* 1989, **24**, 2571